Reconstruction of Complex Permittivity with Neural-Network-Controlled FDTD Modeling*)

E. Eugene Eves[1], Ethan K. Murphy[2] and Vadim V. Yakovlev[3]

[1] The Ferrite Company, Inc., Hudson, NH, USA
[2] Colorado State University, Fort Collins, CO, USA
[3] Worcester Polytechnic Institute, Worcester, MA, USA

The paper discusses further developments of a new modeling-based technique for determining the dielectric properties of materials. Complex permittivity is found with an artificial neural network optimization procedure designed to match the results of 3D FDTD computation and measurement of complex *S*-parameters. Numerical testing demonstrates that the computational part of the method provides the error less than 1% for very wide ranges of dielectric constant and the loss factor. The suggested inverse neural model is capable of efficiently generalizing the training data and reconstructing complex permittivity even when experimental and modeling data are numerically somewhat inconsistent. Special modeling tests validate the technique and confirm a reasonable accuracy in determining the complex permittivity of several liquids at 915 MHz.

Introduction

Knowledge of complex permittivity ($\varepsilon = \varepsilon' - i\varepsilon''$) of materials involved in an application is critical for creating an adequate model and thus for successful system design. The lack of data regarding dielectric constant ε' and the loss factor ε'' of realistic materials to be processed in microwave applicators motivates further development of robust practical techniques of determining complex permittivity. Since ε' and ε'' are calculated given the data on some measurable characteristics, then more difficult tasks may be assigned to a simulator while the experimental part is reduced to an elementary measurement. This approach has been taken in the techniques using the finite element method [1]-[4], the finite-difference time-domain (FDTD) method [5], and finite integration technique [6] for modeling of the entire experimental fixtures.

Further exploring this trend, we have recently developed an innovative method of permittivity reconstruction in which the measured and modeled data are matched by an optimization-type procedure [7], [8]. An artificial neural network (ANN) controls 3D FDTD computation of *S*-parameters of a cavity containing a sample under test, is trained by data from these computations, reads the results of measurements of *S*-parameters, and outputs the reconstructed ε' and ε''. The method works with an arbitrary cavity containing an arbitrarily shaped material sample. In this contribution we describe the outcome of further practice-oriented development of this technique and demonstrate its capabilities of restoring ε' and ε'' in situations where the computed and measured data are numerically inconsistent with each other.

Experimental Setup

In contrast to the resonator-type system employed in the ANN-assisted techniques [2], [7], [8], the experimental component of the present method is realized with a transmission-line fixture (Fig. 1) and is set for measuring the magnitude and phase of the reflection and transmission

*) The full version of this paper is to appear in *Journal of Microwave Power and Electromagnetic Energy*, vol. 41, 2007.

(a) (b)

Fig. 1. The WR975-based two-port fixture (a) and the Teflon container for liquids to be tested (b).

coefficients ($|S_{11}|$, $\angle S_{11}$, $|S_{21}|$, $\angle S_{21}$) at the frequency of interest f_0. A two-port approach allows us working with a set of *S*-parameters at one frequency.

A tested sample is placed inside the fixture. The described experimental setup is particularly convenient for working with liquids or soft substances which are put in a Teflon container (Fig. 1, b). The waveguide fixture standing on a narrow wall is used in order to arrange for the air-sample media interface parallel to the direction of the electric field and thus to make the fixture's parameters not sensitive to an occasional uncertainty in the interface's location.

Network Operations

The radial basis function (RBF) inverse network used in this technique is shown in Fig. 2. For network training and testing, we use information generated in the modeling stage of the method; the latter is powered by the 3D FDTD method. The input layer receives the values of ε' and ε'' for which four *S*-parameters associated with the output layer are computed. Two training techniques, namely backpropagation and the second-order gradient-based algorithm are implemented with the use of the gradient method (iterations from 1 to 200) and the Levenberg-Marquardt method (iterations beyond 200). When the network is sufficiently trained, it is supplied with the values of measured complex *S*-parameters and determines ε' and ε'' of the sample. Further details of the network operations are given in [8].

Numerical Tests and Computational Procedure

Since electromagnetic characteristics of the fixture strongly depend on the complex permittivity of the material in it, it is not feasible to employ the FDTD model with the same parameters for the entire complex permittivity plane. We work with a special two-step procedure allowing us to roughly estimate the position of the unknown (ε', ε'')-point and then focus on the neighborhood of this position in order to find its exact location.

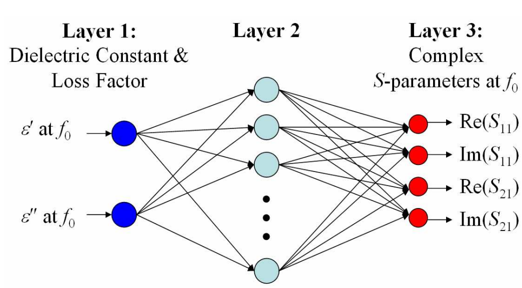

Fig. 2. The RBF network employed in the method.

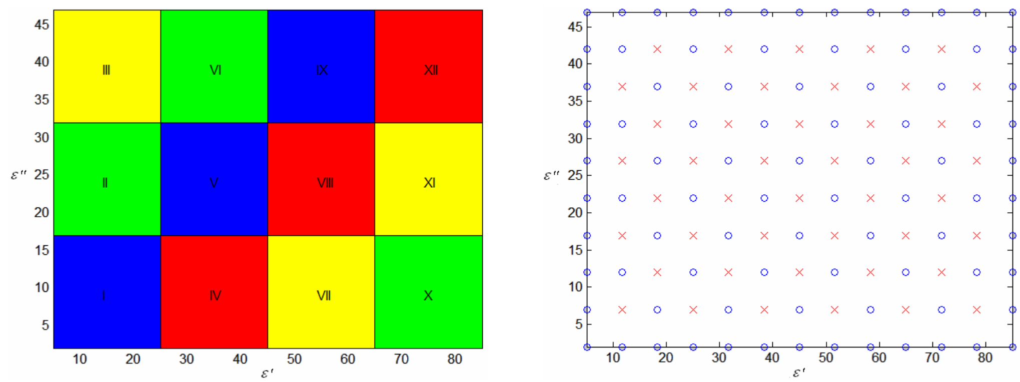

(a) (b)

Fig. 3. 12 domains for identification of anticipated location of the sought point on the ε-plane (a) and the structure of the primary DB (b) used in the described tests (b); (○) and (×) denote training and testing points respectively.

At the first stage, the entire domain of physically possible complex permittivity values is associated with a relatively sparse lattice of the points of the primary database (DB); we work with its structure shown in Fig. 3. Here, the employed FDTD model is built with the cells whose size within the sample is determined by the largest value of its dielectric constant – in the example of Fig. 3, by $\varepsilon' \sim 85$. The DB size is intentionally small, so with the ANN operations described above, we first determine the domain in which the reconstructed (ε', ε'')-point is located. At the second stage, we form the secondary DB surrounding the expected position of the sought point; in the FDTD model, the smallest cell size becomes larger as it is conditioned now by the largest value of ε' in the secondary DB. This approach substantially reduces the computational cost of our method.

The computational component of our technique is implemented as a *MATLAB* code designed as two separate pieces of software: *Database Maker* (*DM*) and *Permittivity Reconstructor* (*PR*); their *MATLAB*-based graphical user interfaces are shown in Fig. 4. Data for training and testing is generated by a model built with the use of the 3D conformal FDTD simulator *QuickWave-3D* (*QW-3D*) [9] which precisely reproduces the geometry of the fixture. The model contains, depending on the dielectric constant of the sample, from 60,000 to 265,000 cells and uses 6 to 25 MB of RAM respectively.

DM governing operations of *QW-3D* is given the name of the related model, the number of FDTD time- steps required to reach steady state, and the parameters of the required DB. *DM* makes a DB and structures it as a single *.mat file. *PR* controls all the network operations: it reads the DM's *.mat file, trains the network with the required accuracy and informs the users on testing results (accuracy of training, elapsed time, etc.). Finally, the user enters the measured values of *S*-parameters in the respective boxes, and *PR* determines the ε' and ε'' of the sample.

Numerical testing of the network performance has shown that the computational method implemented in this technique is robust and highly accurate. For example, using the DBs of 36 on the complex permittivity plane, dielectric constant and the loss factor are reconstructed with errors less than 1% on most of this ε-plane (Fig. 6).

Results of Reconstruction and Their Validation

Table 1 contains the values of complex permittivity reconstructed with the presented technique for four sample liquids in the rectangular (70×70×50 mm) Teflon block with a cylindrical cutout

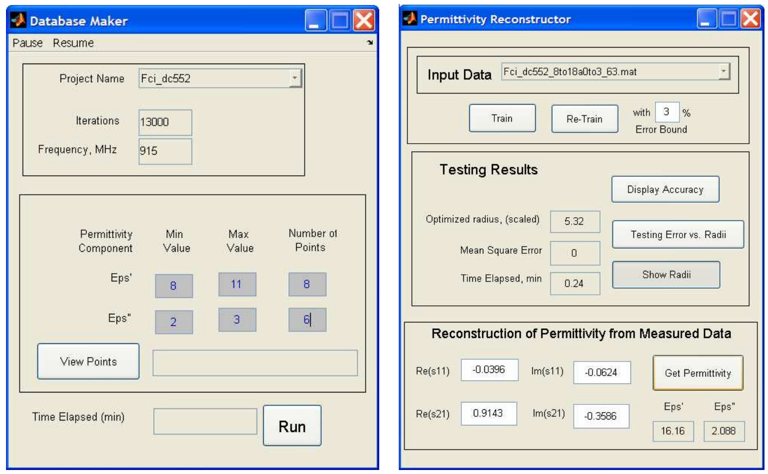

(a) (b)

Fig. 4. General views of the *DM* (a) and *PR* windows (b).

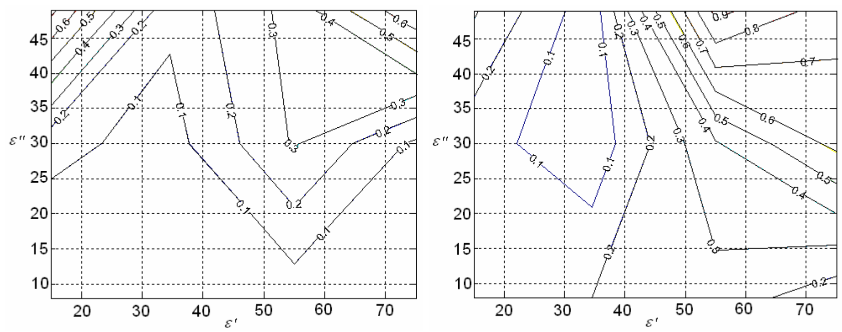

(a) (b)

Fig. 6. Accuracy of reconstruction of dielectric constant (a) and the loss factor (b) – numerical tests with 36-point databases on the ε-plane.

(radius 25 mm, height 40 mm). The primary DB (130 points) was generated once for all samples in accordance with the lattice shown in Fig. 3. For DA and EGW, the secondary DBs (both 63 points) were built around the boundary of domains I and IV (Fig. 7, a) and around domain VII (Fig. 7, b) respectively. Quality of network training by the 63 point secondary DBs is illustrated by Fig. 8: the network demonstrates excellent learning with relatively small data sets in the secondary DBs.

To validate the obtained results, we run the FDTD model with the reconstructed values of ε' and ε'', but for an alternative geometry – the Teflon cup is half-full of liquid. The real and imaginary parts of S-parameters corresponding to this case are measured and compared with the modeling results (see Table 2). The fact that they differ by no more than 0.005, suggests that our method reconstructs complex permittivity with accuracy sufficient for CAD purposes.

The described neural network procedure demonstrates a high level of generalization which is illustrated here by some details in reconstructions of ε' and ε'' for DA. When the experimental values of Re(S_{11}), …, Im(S_{21}) are placed on the S_{11}- and S_{21}-planes of a secondary DB, they represent the point on which the actual (ε', ε'')-pair is mapped from the complex permittivity plane. The fact that the output of our numerical reconstruction is an approximation of the actual value (and thus the approximated point appears at different positions in the S_{11}- and S_{21}-planes) is illustrated by Fig. 9. However, the generalization abilities of the suggested inverse RBF ANN

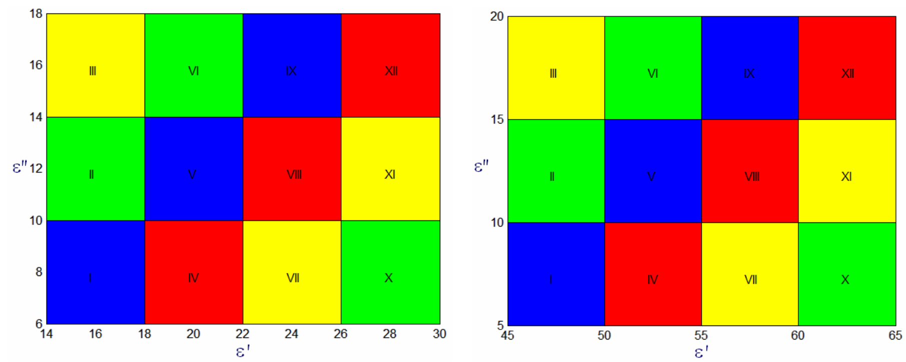

(a) (b)

Fig. 7. 12 domains of the secondary DBs used in the tests for EGW (a) and DA (b).

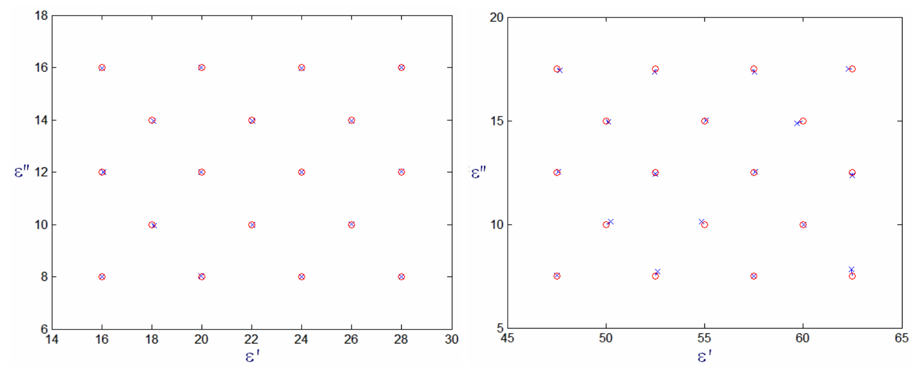

(a) (b)

Fig. 8. ANN responses (×) to the testing points (○) for EGW (a) and DA (b).

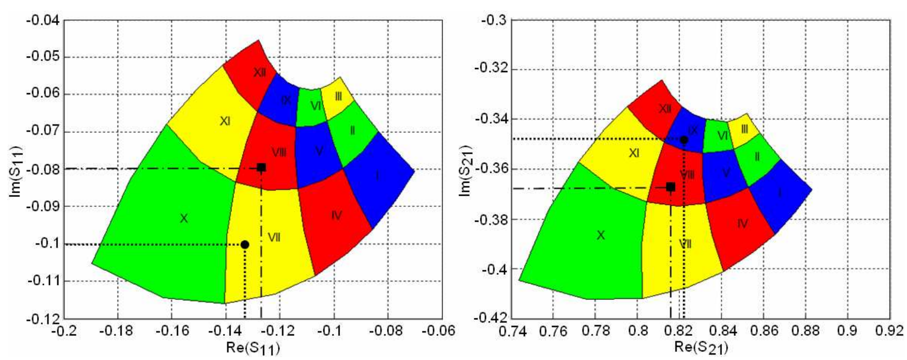

(a) (b)

Fig. 9. 12 domains of the secondary DBs of the ε-plane mapped to the S_{11}- (a) and S_{21}- (b) planes for DA samples; (■) and (●) denote measured and reconstructed points respectively.

Table 1. Reconstructed Complex Permittivity of Tested Liquids at 915 MHz

Sample	Material	Temp., C	ε′	ε″
AC	Acetone	22.5	20.1	0.44
DA	Denatured alcohol	21.0	24.7	10.3
EGW	Ethylene glycol (68%) + water (32%)	22.7	60.8	13.1
SW	Salt water (3.88% NaCl by weight)	22.5	66.0	139.0

Table 2. Validation of the Results in Table 1 – Scenario with Half a Sample

Sample	*S*-Parameter	Re(S_{11})	Im(S_{21})	Re(S_{21})	Im(S_{21})
SW	Measured	-0.036	-0.030	0.923	-0.306
	Modeled (with reconstructed ε)	-0.033	-0.028	0.924	-0.306
EGW	Measured	-0.040	-0.069	0.905	-0.340
	Modeled (with reconstructed ε)	-0.041	-0.073	0.903	-0.345
DA	Measured	-0.023	-0.038	0.935	-0.323
	Modeled (with reconstructed ε)	-0.023	-0.039	0.934	-0.323
AC	Measured	-0.015	-0.035	0.946	-0.321
	Modeled (with reconstructed ε)	-0.013	-0.038	0.945	-0.322

allow it to successfully process numerically dispersed measured data and reconstruct the values of dielectric constant and the loss factor. This is an important advantage that favorably distinguish our approach from the one based on the standard error backpropagation MLP network [2] and makes the entire procedure flexible and robust.

Conclusions

It has been demonstrated that the novel neural-network-based FDTD-backed technique of complex permittivity reconstruction is capable of efficiently determining the dielectric constant and the loss factor of diverse materials placed in a transmission-line-type cavity. The experimental part is reduced to measuring the reflection and transmission coefficients of the systems. The technique is frequency- and cavity-independent, applicable to the samples and fixtures of arbitrary configuration. For materials which can take some predefined form, the computational cost of the method is very insignificant. Since the underlying full-wave modeling technique easily handles the arbitrary sample/fixture geometry and since the ANN technology is capable of robust generalizing the measured data and adjusting to the physical characteristics of the cavity, our method is a convenient and efficient technique of complex permittivity reconstruction well suited to practical applications.

References

[1] R. Coccioli, G. Pelosi, and S. Selleri, Characterization of dielectric materials with the finite-element method, *IEEE Trans. Microwave Theory Tech.*, vol. 47, no 10, pp. 1106-1112, 1999.

[2] R. Olmi, G. Pelosi, C. Riminesi and M. Tedesco, A neural network approach to real-time dielectric characterization of materials, *Microwave Opt. Tech. Let.*, vol. 35, no 6, pp. 463-465, 2002.

[3] K.P. Thakur and W.S. Holmes, An inverse technique to evaluate permittivity of material in a cavity, *IEEE Trans. Microwave Theory Tech.*, vol. 49, no 10, pp. 1129-1132, 2001.

[4] M. Santra and K.U. Limaye, Estimation of complex permittivity of arbitrary shape and size dielectric samples using cavity measurement technique at microwave frequencies, *IEEE Trans. Microwave Theory Tech.*, vol. 53, no 2, pp. 718-722, 2005.

[5] B. Wäppling-Raaholt, and P.O. Risman, Permittivity determination of inhomogeneous foods by measurement and automated retro-modeling with a degenerate mode cavity. *Proc. 9th Conf. Microwave and HF Heating, Loughborough, U.K., Sept. 2003*, pp. 181-184.

[6] M.E. Requena-Pérez, A. Albero-Ortiz, J. Monzó-Cabrera, and A. Díaz-Morcillo, Combined use of genetic algorithm and gradient descent optimization methods for accurate inverse permittivity measurement, *IEEE Trans. Microwave Theory Tech.*, vol. 54, no 2, pp. 615-624, 2006.

[7] E.E. Eves, P. Kopyt and V.V. Yakovlev, Determination of complex permittivity with neural networks and FDTD modeling, *Microwave Opt. Tech. Let*. vol. 40, no 3, pp. 183-188, 2004.

[8] V.V. Yakovlev, E.K. Murphy and E.E. Eves, Neural networks for FDTD-backed permittivity reconstruction, *COMPEL*, vol. 24, no 1, pp. 291-304. 2005.

[9] QuickWave-3D™, 1996-2006, QWED Sp. z o. o., ul. Piêkna 64a m 11, 00-672 Warsaw, Poland, http: //www.qwed.com.pl/.